Developmental Biology **211,** 11–26 (1999)
Article ID dbio.1999.9276, available online at http://www.idealibrary.com on IDEAL®

the Body Axis and the Lateral Asymmetry of the Mouse Embryo during Early Organogenesis

Bruce P. Davidson,* Simon J. Kinder,* Kirsten Steiner,* Gary C. Schoenwolf,† and Patrick P. L. Tam*

**Embryology Unit, Children's Medical Research Institute, Locked Bag 23, Wentworthville, New South Wales 2145, Australia; and †Department of Neurobiology and Anatomy, University of Utah School of Medicine, 50 North Medical Drive, Salt Lake City, Utah 84132*

The node of the mouse gastrula is the major source of the progenitor cells of the notochord, the floor plate, and the gut endoderm. The node may also play a morphogenetic role since it can induce a partial body axis following heterotopic transplantation. The impact of losing these progenitor cells and the morphogenetic activity on the development of the body axes was studied by the ablation of the node at late gastrulation. In the ablated embryo, an apparently intact anterior–posterior body axis with morphologically normal head folds, neural tube, and primitive streak developed during early organogenesis. Cell fate analysis revealed that the loss of the node elicits *de novo* recruitment of neural ectoderm and somitic mesoderm from the surrounding germ-layer tissues. This leads to the restoration of the neural tube and the paraxial mesoderm. However, the body axis of the embryo was foreshortened and somite formation was retarded. Histological and gene expression studies reveal that in most of the node-ablated embryos, the notochord in the trunk was either absent or interrupted, and the floor plate was absent in the ventral region of the reconstituted neural tube. The loss of the node did not affect the differentiation of the gut endoderm or the formation of the mid- and hindgut. In the node-ablated embryo, expression of the *Pitx2* gene in the lateral plate mesoderm was no longer restricted to the left side but was found on both sides of the body or was completely absent from the lateral plate mesoderm. Therefore, the loss of the node results in the failure to delineate the laterality of the body axis. The node and its derivatives therefore play a critical role in the patterning of the ventral neural tube and lateral body axis but not of the anterior–posterior axis during early organogenesis.

Key Words: **body axis; laterality; gene expression; node; notochord; mouse embryo.**

INTRODUCTION

Gastrula-stage embryos of zebrafish, *Xenopus*, the bird, and the mouse are anatomically different from one another and they employ different morphogenetic strategies for the formation of germ layers (reviewed by Arendt and Nübler-Jüng, 1996; Slack, 1994). Despite these differences, a similar body plan (or fate map) is found among these embryos at early gastrulation (Lawson *et al.*, 1991; Lawson and Pedersen, 1992; Tam and Behringer, 1997) and an essentially conserved repertoire of gene activity may be involved with the regulation of morphogenesis and lineage specification during gastrulation (Lemaire and Kodjabachian, 1996; Tam and Quinlan, 1996; Bally-Cuif and Boncinelli, 1997).

Experimental studies have revealed that the inductive activity of a specific group of cells in the vertebrate gastrula may be critical for the organization of the body pattern. In the classic experiments of Spemann and Mangold (1924), the dorsal lip of the blastopore of the amphibian embryo, when transplanted heterotopically, was able to organize a secondary embryo complete with an induced neuraxis. Consequently, this structure is accorded the role of an organizer of the body plan (reviewed by Gilbert and Saxen, 1993; Harland and Gerhart, 1997). A functionally equivalent organizer exists in the embryonic shield (zebrafish: Ho, 1992; Shih and Fraser, 1996) and Hensen's node (bird: Izpisúa-Belmonte *et al.*, 1993; Dias and Schoenwolf, 1990; Storey *et al.*, 1992). In the mouse, the node of the late gastrula, like the organizer in other vertebrate gastrulae, can induce the formation of a secondary body axis by

0012-1606/99 $30.00

patterning the host tissues into a new neural tube flanked by paraxial tissues after heterotopic transplantation (Beddington, 1994; Tam *et al.*, 1997b). However, the induced axis lacks the structures that are characteristic of the anterior (rostral) neural tube, raising the possibility that the node may not contain the organizing activity for the entire axis (Beddington and Robertson, 1999).

The node of the mouse embryo has been shown to be the primary source of the progenitors for the notochord, the floor plate of the neural tube, and the gut endoderm (Beddington, 1994; Sulik *et al.*, 1994; Tam and Beddington, 1987, 1992). In several mutants, defects in body organization have been attributed to loss of patterning activity due to the defective node and to the loss of notochord which degenerates as the embryo develops (*T:* Rashbass *et al.*, 1994; Conlon *et al.*, 1995; Herrmann, 1995; *Shh:* Chiang *et al.*, 1996; *no turning:* Melloy *et al.*, 1998). In the *Hnf3β*-null mutant embryos, both the node and the notochord are absent. However, in these notochordless embryos, a rudimentary body axis which appears to have a normal anterior–posterior pattern is formed (Ang and Rossant, 1994; Weinstein *et al.*, 1994; Dufort *et al.*, 1998). This may suggest that, in the *Hnf3β* mutant, the notochord and the node are not critical for the proper anterior–posterior development of the body axis at least up to the stage of organogenesis.

The role of the organizer and its derivatives has been tested using an embryological approach by surgical ablation of the organizer of the gastrula-stage embryo. For example, extirpation of the embryonic shield region of the zebrafish 50%-epiboly stage gastrula results in embryos (80% of cases) missing the head and trunk notochord. An apparently normal neural tube is formed although the axis is distorted and foreshortened, and somites are often fused medially (Shih and Fraser, 1996). Excision of the blastopore lip of Stage 10 *Xenopus* gastrula results in the loss of the notochord but the embryo forms a normal body axis (Cooke, 1985). Notochordless embryos that are produced by UV irradiation display a malformed and shortened axis but show proper anterior–posterior polarity in the neural tube (Cooke, 1985; Clarke *et al.*, 1991). In the chick embryo, at least two organizer derivatives, the notochord and the floor plate, could be reconstituted when Hensen's node and the adjacent part of the primitive streak are ablated at stages preceding notochord formation (Psychoyos and Stern, 1996; Yuan *et al.*, 1995a,b). In the late-streak stage mouse gastrula, extirpation of an embryonic fragment containing the node and the adjacent germ-layer tissues apparently has no effect on the morphology of the embryonic axis other than a reduction in somite number (Snow, 1981). Whether the notochord is missing in these ablated mouse embryos is not known. Nevertheless, the outcome of these ablation experiments performed on a variety of vertebrate embryos suggests that either the necessary axial information is already acquired by the embryonic tissues at gastrulation so that an axis will develop autonomously in the absence of the organizer or the loss of the organizer and the notochord progenitors contained therein has been restored by tissue regeneration.

In the present study, experiments were designed to address two questions: (1) Do the body axes develop normally after the ablation of the node at late gastrulation and (2) is axis development in the node-ablated embryo accompanied by the reconstitution of the notochord and floor plate?

MATERIALS AND METHODS

Embryo Dissection, Manipulation, and Culture

Embryos at the late gastrulation stages were dissected from 7.5-day pregnant ARC/s mice. Only embryos at the early-allantoic-bud stage (Downs and Davies, 1993) were used for this study (Figs. 1A–1C). In these embryos, the primitive streak has extended to its full length from the allantoic bud to the node at the distal tip of the egg cylinder. When viewed under the dissecting microscope, node tissues display a more compact and translucent appearance. Anterior to the node, the embryonic tissues are distinctly organized into separate germ layers. Posteriorly, the node is contiguous with the primitive streak. In the experimental group, a 50 by 50-μm tissue fragment containing the node and some tissues in the adjacent germ layers was excised from the distal tip of the embryo (the node-ablated embryo, Fig. 1C), using electrolytically polished alloy metal needles or finely drawn glass needles. For the controls, sham

FIG. 1. (A–C) The three types of manipulation performed: sham cut (white arrows) to the lateral germ layer (lateral cut, A) or to the node (node split, B) and node ablation (node ablated, C). A wedge of embryonic tissue containing the node was excised by making two cuts at the anterior and the posterior border of the node. The wound (asterisk in C) left after the removal of tissues always gaped open (F, I), giving the impression that more than the amount of the tissue contained in the fragment has been removed. In control embryos in which a transverse slit was made in the node (node split), a similar splaying of the wound was also observed (E). The extent of node ablation was studied by the expression of genes that are associated with the node. The control and node-split embryos maintained normal expression of the *Hnf3β* (D, E) and *chordin* (G, H) activity, but in the ablated embryo (F, I), the activity was absent in the germ layer and the primitive streak tissue left after ablations, but normal expression in the anterior mesoderm remains. Bar, 100 μm for A–I. (J–O) The expression of *Hnf3β* and *Lim1* genes after manipulation and 5–6 h of culture. (J) Lateral-cut and (K) node-split control embryos expressing *Hnf3β* in the node and anterior mesendoderm. (L) Node-ablated embryo showing (i) *Hnf3β* expression in the presumptive node (arrow) and (ii) no expression in the tissue (double arrows) anterior to the primitive streak. (M) Lateral-cut and (N) node-split control embryos expressing *Lim1* in the node, anterior midline, and lateral mesoderm. (O) Node-ablated embryos showing (i) *Lim1* expression (arrow) and (ii) no expression (double arrows) in the presumptive node region. Bar, 250 μm for J–O.

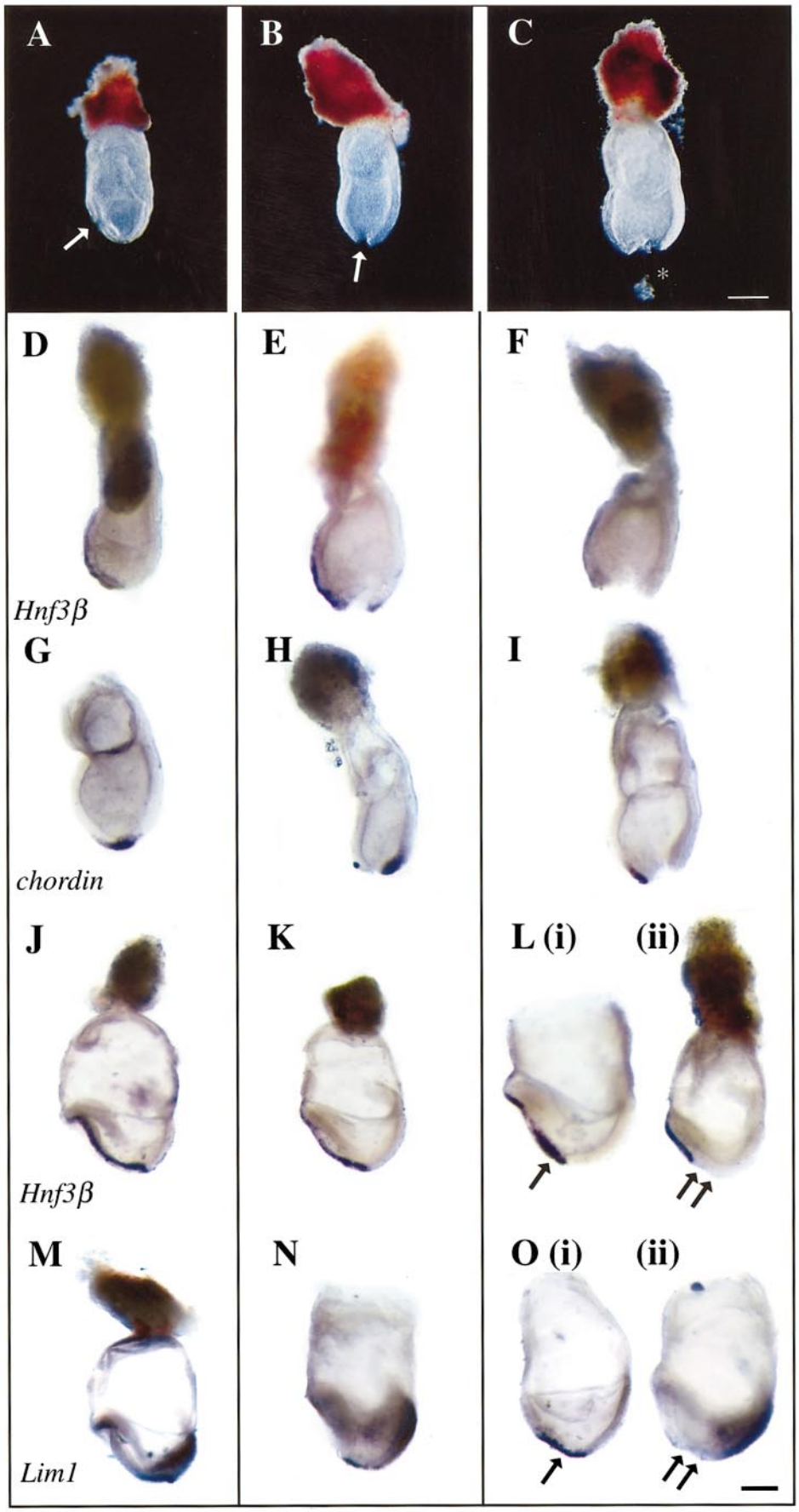
CONTROL
NODE-SPLIT
NODE-ABLATED
A
B
C
*
D
E
F
Hnf3β
G
H
I
chordin
J
K
L (i)
(ii)
Hnf3β
M
N
O (i)
(ii)
Lim1

operations were performed by slicing either through the germ layers in the lateral region (lateral cut, Fig. 1A) or through the distal tip of the embryo, which results in the splitting of the node (node split, Fig. 1B). Following the manipulation, the embryos were cultured for up to 24 h in culture medium containing 75% rat serum in Dulbecco's modified Eagle's medium (Sturm and Tam, 1993).

Tracing Tissue Fate in the Node-Ablated Embryo

In the allantoic-bud stage embryos, cells in the ectoderm and mesoderm on either side of the axis and lateral to the node were labeled separately with the carbocyanine dyes, DiI (1,1′-dioctadecyl-3,3,3′,3′-tetramethyl indocarbocyanine perchlorate) and DiO (3,3′-dioctadecyl oxacarbocyanine perchlorate; Molecular Probes). Dye crystals were dissolved in 100% ethanol and the resulting solution was diluted 1:20 in 0.2 M sucrose to give the working solution. To label cells in the embryos, a small volume of dye solution was microinjected into the germ layers using micropipettes operated by a de Fonbrune pressure pump (Alcatel) and micromanipulators (Leica). Groups of cells at about 50 μm from the midline on both sides of the node were labeled (Fig. 2A). Two types of manipulation were then performed. In one group, the distal region of the embryo was surgically extirpated (node ablated) while in the other group, a transverse cut was made to the distal tip of the embryo (node split). The operated embryos were then cultured *in vitro*. At various time points (2, 5, 10, and 26 h), the labeled embryos were harvested and fixed in 4% paraformaldehyde overnight at 4°C. Fixed embryos were mounted in phosphate-buffered saline on glass depression slides and were examined under a fluorescence microscope (Leica DMLB) using rhodamine (for DiI) and FITC (for DiO) excitation and transmission filter sets. The images were captured by a CCD camera with intensifier (Panasonic WV-CL 700/A) and processed digitally using Leica Q500MC image processing and analysis software. Labeled embryos were postfixed in 4% paraformaldehyde, embedded in OCT medium (Tissue-Tek), sectioned at 10–12 μm at −20°C using a cryomicrotome (Microm HM500OM). The sections were mounted on glass slides, washed once in phosphate-buffered saline to remove the OCT medium, and examined by fluorescence microscopy.

Whole-Mount in Situ Hybridization and Histology

Experimental and control embryos were collected from the culture and fixed overnight in 4% paraformaldehyde at 4°C. The fixed embryos were rinsed in phosphate-buffered saline and the morphology of the midline tissues, the somites, and the neural tube was examined. The specimens were then processed for mRNA *in situ* hybridization, according to the protocol of Wilkinson and Nieto (1993) with some modifications. The riboprobes were synthesized using the Ampliscribe kit (Epicentre Technologies) and labeled with digoxigenin-11–UTP (Boehringer Mannheim). For the hybridization steps, SDS (instead of Chaps), 5× SSC, and 0.2 μg/ml probe were used in the hybridization solution. No RNase digestion was performed after hybridization. Posthybridization washes were done at 70°C, at high stringency and without the use of formamide. After whole-mount *in situ* hybridization, selected embryos were postfixed in 4% paraformaldehyde and embedded in paraffin wax. Serial 7- to 8-μm sections of the embryo were examined either unstained under differential interference optics (Leica) or after counterstaining with Nuclear Fast red.

Analysis of Tissue Differentiation and Morphogenesis

To determine the extent of tissue extirpation, embryos were examined for the activity of genes that are normally expressed in the node and the primitive streak. The expression of *Hnf3β*, *chordin*, *Lim1*, and *T* was studied in the node-ablated embryos immediately after the manipulation and at 5–6 h after ablation to assess the development of the midline mesendoderm and the node, and the expression of *Otx2* and *Hoxb1* was examined to reveal the general anterior–posterior pattern in the germ layers.

The development of the axial tissues was assessed by studying the expression of *Hnf3β*, *Shh*, and *T* genes. Embryos showing different patterns of gene activity were grouped into three categories: complete, partial, and absent formation of axial tissues. Node-ablated embryos were also examined for gene expression by *in situ* hybridization of mRNA to reveal the development of the somite (*Mox1*), the gut endoderm (*Shh*), and the primitive streak (*T*). The asymmetry of the lateral plate mesoderm and the differentiation of the head-fold ectoderm were assessed by the expression of *Pitx2*. Double *in situ* hybridization for *Pitx2* and *T* mRNAs was performed on some embryos for a correlation of lateral tissue asymmetry and the differentiation of the axial mesendoderm.

RESULTS

Gene Expression Reveals That the Node Was Ablated

In the control (intact and lateral-cut) and the node-split embryos, cells expressing the *Hnf3β* transcript were found in the head process and the node (Figs. 1D and 1E) while cells expressing *chordin* were localized mainly in the node and the midline tissue immediately anterior to the node (Figs. 1G and 1H). The control embryos also expressed *T* transcript in the primitive streak and the node and *Lim1* transcript in the node and anterior midline mesendoderm (data not shown). Most of the ablated embryo displayed complete absence of *Hnf3β*, *chordin*, *T*, and *Lim1* in the germ-layer tissues around the wound (Table 1A, Figs. 1F and 1I; and data not shown). Therefore, the microsurgical operation has effectively ablated the entire node and the neighboring germ-layer tissues in the majority of the experimental embryos. Some residual *Hnf3β*-, and *chordin*-expressing tissue was found on the posterior side (the primitive streak side) of the wound in 21% of the node-ablated embryos (Table 1A). However, the significant reduction in the *Hnf3β*- and *chordin*-expressing tissues suggests that most of the node cell population has been removed.

The Node Is Not Reconstituted after Ablation

In the control (intact and node-split) embryos after 5–6 h of *in vitro* culture (at the early head-fold stage), *Hnf3β*, *Lim1*, *T*, and *chordin* genes are expressed in the node and the anterior mesendoderm associated with the head folds (Figs. 1J, 1K, 1M, and 1N, and data not shown). In the node-ablated embryos, the majority shows no expression of the four genes in the tissues that healed the wound but

TABLE 1

Analysis of Gene Expression and the Development of Mouse Embryos Following the Ablation of the Node and Adjacent Germ-Layer Tissues

A. Extent of ablation (t = 0 h)

Gene activity in the node region	Control (intact, lateral cut, and node split)	Node ablated	
		Absent	Residual
T	15	18	0
Hnf3β	22	21	7
Chordin	29	15	9
Lim1	8	7	0
Total		61 (79%)	16 (21%)

B. Gene activity in response to the ablation (t = 5–6 h)

Gene activity in the node region	Control (intact, lateral cut, and node split)	Node ablated	
		Absent	Expressed
T	11	11	0
Hnf3β	11	17	9 (5)[a]
Chordin	9	4	0
Lim1	9	10	6
Total		42 (74%)	15 (26%)
Otx2	14		9
Hoxb1	3		9

C. Gene expression in the axial tissues during organogenesis (t = 24 h)

Gene activity in the node region	Intact	Lateral cut	Node split	Node-ablated		
				Absent	Partial	Complete
T	5	3	6	7 (54%)	5 (38%)	1 (8%)
Hnf3β	4	4	7	11 (44%)	5 (20%)	9 (36%)
Shh	3	4	8	8 (57%)	4 (29%)	2 (14%)
Total				26 (50%)	14 (27%)	12 (23%)
Somite number	nd	4.8 ± 0.3 (32)[b]		3.8 ± 0.4 (26)[c]	4.2 ± 0.6 (14)	4.3 ± 0.7 (12)

Note. Data given are numbers of embryos. Examples of *in situ* hybridization results for t = 0 and 5–6 h are shown in Fig. 1. Axis development was assessed by *T, Shh,* and *Hnf3β* expression. Embryos were divided into three categories based on the expression patterns of these genes in the trunk region of the embryo. Embryos that expressed these genes in the entire axis were regarded as having a completely formed midline. Those embryos that displayed gene activity in the axial tissues only in the head and occasionally in regions juxtaposed to the primitive streak were regarded as having a partially formed axial structure. Last, embryos that did not display any gene activity are lacking midline tissue differentiation. Examples of the three categories of axis development are shown in Fig. 3.

[a] Patchy expression of *Hnf3β* was detected in the tissues surrounding the ablation.

[b] Somite number for control embryos was based on pooled embryos of the lateral-cut and node-split controls.

[c] Significant difference from control in somite number ($P < 0.05$) by Mann–Whitney test.

appropriate *Hnf3β* and *T* expression in the anterior midline mesendoderm and *T* expression in the primitive streak was maintained (Figs. 1L(ii) and 1O(ii), Table 1B).

In four embryos whose wound had healed, *Hnf3β* activity was detected in the tissues at the anterior end of the primitive streak (Fig. 1L(i)). In five embryos that had not healed the ablation, patchy expression of *Hnf3β* activity was found in the tissue at the edge of the wound (data not shown). Reexpression of the *Lim1* transcripts was found in the healed tissues in the remaining six node-ablated embryos (Fig. 1O(i)). Altogether, about 26% of the node-ablated embryos showed expression of the *Hnf3β* or *Lim1* gene in the healed tissues (Table 1B). This percentage is comparable to the 21% of embryos that retained residual *Hnf3β*- or *chordin*-expressing tissue immediately after ablation, suggesting that the *Hnf3β*- or *Lim1*-expressing tissues in the

TABLE 2
The Allocation of Cells from the Lateral Germ Layers to Embryonic Tissues Following the Ablation of the Node

Time after manipulation (h)	Node split		Node ablated	
	Wound healed? (*N*)	DiO/DiI-labeled cells	Wound healed? (*N*)	DiO/DiI-labeled cells
2	Yes (2)	Separate	No (3)	Separate
			Yes (1)	Merged
5	Yes (2)	Lateral to the node	Yes (4)	On either side of the healed tissues
			Yes (1)	Mixed in the healed tissues
10	Yes (2)	Paraxial tissues	Yes (3)	Midline and paraxial tissues
		Hindbrain level (1)		Hindbrain level (2)
		Hindbrain to trunk (1)		Hindbrain to trunk (1)
26			No (2)	Later to the hiatus (2)

	Distribution of DiI/DiO-labeled cells								
	Node split				Node ablated				
	N	Crm	Som	Nt	*N*	Crm	Som	Nt	Ncd
Intact axis	9	4 (2)[a]	4 (3)[a]	1 (1)[a]	17	6 (2)[a]	2 (2)[a]	11 (5)[a]	(1)[a]
Somite number (*N*)			9.7 ± 0.5 (9)[b]				6.1 ± 0.5 (11)[b]		
Split axis	1	0	0	1	8	2	1	6	0
Somite number (*N*)			11 (1)				5.6 ± 0.8 (7)		

[a] Number in parentheses shows the number of specimens analyzed histologically by fluorescence microscopy.
[b] Significant difference at $P < 0.05$ by Mann–Whitney test. Abbreviations: *N*, number of embryos analyzed; Crm, cranial mesoderm; Som, somites, Nt, neural tube; Ncd, notochord.

node at 5–6 h might be derived from the residual tissues, rather than *de novo* reconstitution of the node.

Germ-Layer Tissues Are Recruited to the Midline Structure after Node Ablation

Cells in the ectoderm and mesoderm lateral to the node were labeled separately with two carbocyanine dyes. The distribution of these two cell populations was then followed for up to 26 h of *in vitro* development (Table 2). In the node-split control embryos, these two cell populations remained separated when the embryos were examined at 2 and 5 h ($n = 2$ for each time point) of *in vitro* development (Figs. 2A and 2B). By 10 h, the labeled populations were found in the paraxial mesoderm on either side of the body axis in the cranial and the trunk regions ($n = 2$, data not shown). Of the 10 embryos examined after 26 h of culture, 9 developed an intact axis and the labeled cells were found mainly in the paraxial mesoderm at the level of the hindbrain and in the somites. The two differently labeled populations colonized the paraxial mesoderm on opposite sides of the body axis (Fig. 2C). In one embryo, DiI- and DiO-labeled cells were found separately in the contralateral half-neural tubes lining the edge of split body (Table 2). Labeled cells derived from the germ layers lateral to the node of the late gastrula therefore contribute mainly to the paraxial mesoderm of the embryo during early organogenesis.

In the node-ablated embryos, labeled cells lateral to the ablation converged toward the midline (2 h after ablation, $n = 4$, Fig. 2D) and some were found in the tissues that filled the wound (Fig. 2E). After 5 and 10 h of culture, labeled cells were displaced farther toward the midline (Fig. 2F; Table 2) than in the split-node controls (Fig. 2B) and were found in the neural plate. Of the 25 node-ablated embryos examined after 26 h of culture, 17 (68%) had an intact body axis with a complete neural tube. In these embryos, labeled cells from the germ layers previously flanking the ablated region contributed predominantly to the neural tube (Fig. 2G) as well as to the paraxial mesoderm (Fig. 2H, Table 2). Contribution to the axial structure that resembled the notochord was observed in only one embryo (Table 2). The remaining 8 embryos displayed a midline hiatus which was flanked on either side by a half-neural tube and one row of somites. In these embryos, labeled cells were also found mostly in the neural tube and the paraxial mesoderm (Table 2).

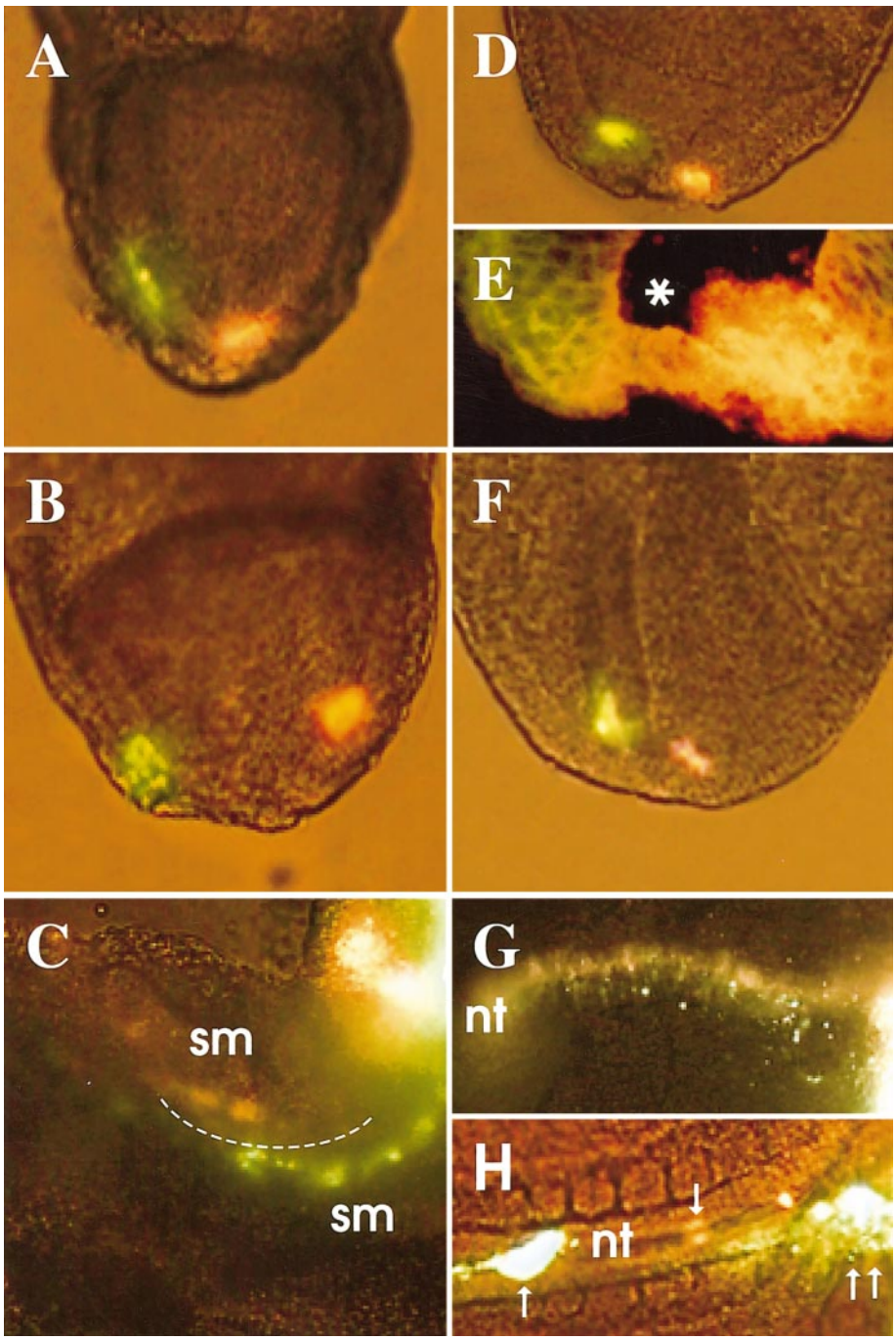

FIG. 2. Tracing the fate of germ-layer tissues in the node-ablated embryo. (A, B) Control node-split embryo showing cells in different sides of the node region that were labeled separately with DiO and DiI (A, 2 h and B, 5 h after labeling). (C) Control node-split embryos examined 25–26 h after labeling. Labeled cells are found in the paraxial mesoderm of the hindbrain and the trunk (broken line marks the body axis with anterior to the right; sm, somites). (D, E, F) Node-ablated embryo (2 h after labeling) showing the labeled cells converging toward the midline (D) and in the tissues bridging the wound (E) and the close proximity of the two labeled populations to the midline in the prospective hindbrain of the head folds (F; 5 h after labeling). (G, H) Node-ablated embryos after 25–26 h of culture (anterior end of the embryo to the right) showing (G) the intermingling of labeled cell populations in the neural tube (nt) and (H) distribution of the labeled cells in the anterior somites (double arrows) and the neural tube (single arrows).

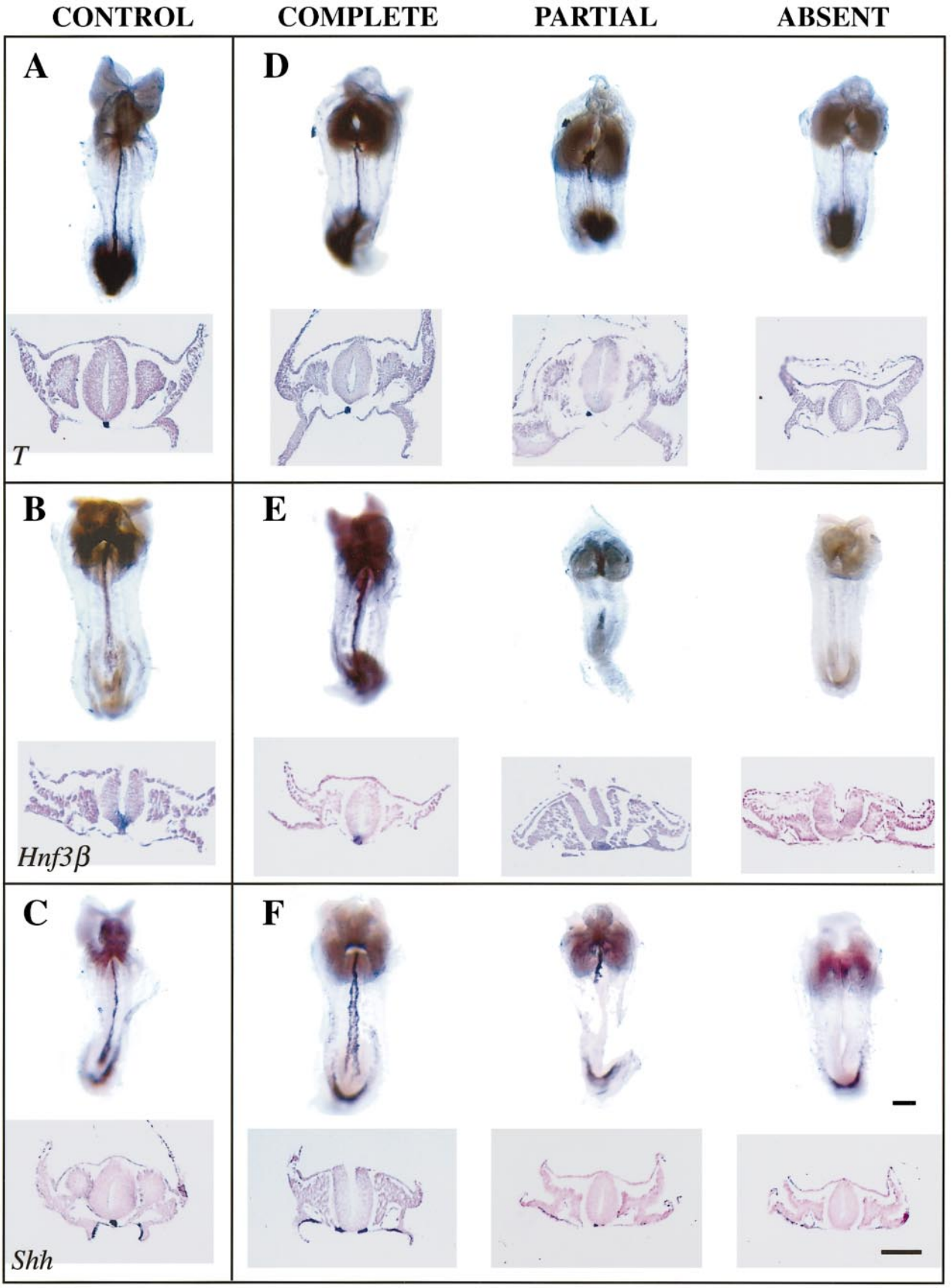

Anterior–Posterior Axis Development Is Not Significantly Affected but No Floor Plate Differentiates in the Notochordless Embryo

Otx2 and *Hoxb1* genes were also examined in 18 node-ablated embryos 5–6 h after ablation (Table 1B). The *Otx2* transcripts were localized to the head-fold region of the embryo and the *Hoxb1* transcripts were found in the germ layers in the posterior region of the embryo (data not shown). This anterior–posterior regionalization of *Otx2* and *Hoxb1* expression was the same as that of the control embryos.

After 24 h of *in vitro* development, the control (intact, lateral-split, and node-split) embryos developed to the early-somite stage, with axial tissues expressing *T, Shh,* and *Hnf3β* activity; cephalic neural folds that are partitioned into the major brain regions; an elongated neural tube; an average of 4.8 pairs of somites; a beating heart; and well-developed foregut and hindgut portals (e.g., Figs. 3A–3C and 4C–4F; Table 1C).

About 65% of the node-ablated embryos formed a complete body axis and developed head folds showing the prospective brain regions (Figs. 3D–3F). Normal expression of the *Pitx2* gene was found in the forebrain ectoderm and the underlying mesenchyme (Figs. 4G–4J). Histological examination reveals the presence of an intact neural tube in the trunk (Figs. 3D–3F). The cells in the posterior neuropore and the primitive streak also expressed normal levels of *T* mRNA (Fig. 3D). The gut endoderm expressed bilateral *Shh* activity (Fig. 3F) and gut invaginations were formed (Figs. 3D–3F and 4G–4J). Some node-ablated embryos failed to repair the ablation and displayed a midline hiatus in the trunk (e.g., Figs. 3F, absent, and 4I). The node-ablated embryos generally formed fewer somites (Tables 1C, 2, and 3). In some embryos, somites were less condensed and some fused medially underneath the neural tube, which sometimes did not fuse or elongate to the same extent as in the control embryos.

About 77% of the node-ablated embryos display no expression of *T, Shh,* or *Hnf3β* activity or an interrupted expression in the axial tissue of the trunk after whole-mount *in situ* hybridization (Figs. 3D–3F, absent and partial; Table 1C). Histological examination of the embryos with "absent" expression revealed that no axial structure resembling the notochord was found underneath the neural tube (Figs. 3D–3F). Since *Shh* activity was detected normally in the gut endoderm, the lack of *Shh* expression in the midline was due to the absence of the axial tissues and not the failure to activate transcription. Despite the formation of an intact neural tube, no expression of *Hnf3β* activity that signifies the prospective floor plate was found in the ventral neural tube in these notochordless embryos. In the embryos showing partial gene expression, *T, Shh,* and *Hnf3β* activity was expressed in the midline mesendoderm of the head folds and in a notochord-like structure underneath the neural tube (Figs. 3D–3F, partial). However, this notochord-like structure was interrupted along the trunk and was often distorted in shape and displaced laterally. *Hnf3β* expression was absent from the ventral part of the neural tube in embryos with a partial axial gene expression, suggesting that the prospective floor plate was not formed when only a partial axial notochord-like structure was present. In about 23% of the node-ablated embryos (Table 1C), a single axial structure that expressed *T, Shh,* and *Hnf3β* activity that resembles the notochord was found underlying the neural tube (Figs. 3D–3F, complete). In some embryos, *T*- and *Shh*-expressing midline tissues appeared to be duplicated and two parallel notochord-like structures were formed (Fig. 3F, complete). *Hnf3β* transcripts were present in the ventral part of the neural tube. These node-ablated embryos also displayed normal axial length and somite number. It is likely that these embryos were derived from those that showed residual node-specific gene activity at 0 and 5–6 h after node ablation.

The Asymmetric Pitx2 Expression in the Lateral Plate Mesoderm Is Disrupted When the Notochord Is Absent

In the early-somite-stage embryo, transcripts of the *Pitx2* gene are expressed in lateral plate mesoderm (LPM) on the left side of the body. The expression initially extends to the entire length of the mesoderm (Fig. 4A) and subsequently is restricted to the lateral plate mesoderm of the upper trunk (Fig. 4B). Embryos that developed *in vitro* during neurulation and early organogenesis displayed randomized expression of the *Pitx2* transcript (Table 3, Intact control). *Pitx2* was expressed in the left LPM of about 47% of the cultured

FIG. 3. Differentiation of the axial tissues in (A–C) control and (D–F) node-ablated embryos revealed by the expression of *T* (A, D), *Hnf3β* (B, E), and *Shh* (C, F) in whole-mount and sectioned specimens. The control embryos display normal development of the somites, the neural tube, and the notochord (A–C) and the floor plate (B). In the node-ablated embryos (D–F), three categories of axial development were found. Embryos showing full expression of the three genes in the midline tissues (the complete group) form an intact neural tube and properly organized somites, lateral plate mesoderm, and gut endoderm. Histological examination reveals the presence of a morphologically distinct notochord and, by the expression of *Hnf3β,* the differentiation of the floor plate (E, complete). An example of duplicated *Shh*-expressing presumptive notochord is shown (F, complete). Some node-ablated embryos show disjointed segment of gene expression in the midline tissues (the partial group). Expression is usually present in the axial tissues of the head folds and extends posteriorly to level of the first one or two somites. Expression is missing in the trunk and reappears near the primitive streak. About 50% of the node-ablated embryos do not show any expression of the three genes in the midline (the absent group). Neural tube and somite development appear normal, but no axial structure resembling the notochord is formed underneath the neural tube and no floor plate differentiation is observed. Bars, 50 μm.

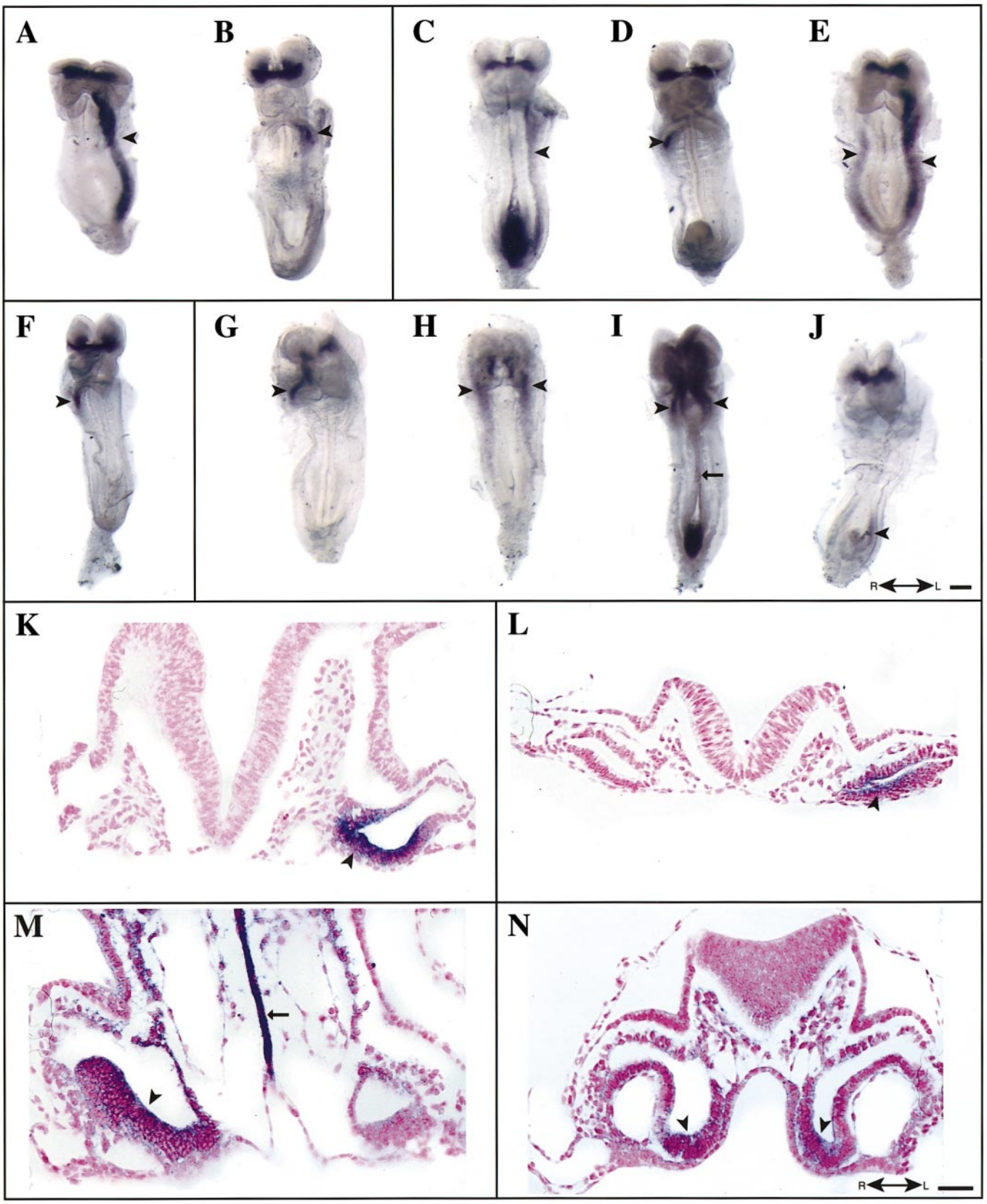

TABLE 3

The Expression of *Pitx2* Transcripts in Lateral Plate Mesoderm of the Experimental and Control Mouse Embryos

	N	Somite No. (mean ± SEM)	*Pitx2* expression in LPM (No. of embryos)			
			Left	Right	Left and right	No expression
In vivo 8.5-day embryo	23	5.7 ± 0.4 (23)	23	0	0	0
7.5 day + 26–28 h *in vitro*						
Intact control[a]	26[b]	7.2 ± 0.5 (26)	13	2	8	3
Split node[c]	21[d]	7.3 ± 0.2 (21)	5	6	7	3
Node ablated[e]	28[f]	5.6 ± 0.3 (25)	1	3	14	10

Note. LPM, lateral plate mesoderm; *N*, number of embryos analyzed.

[a] Significant difference from *in vivo* embryos for the *Pitx2* expression pattern ($\chi^2 = 17.5$, $P < 0.01$ by 2×4 χ^2 test).

[b] 14 embryos were cohybridized with *T* riboprobe, all showed normal expression in axial tissues.

[c] No significant different from the intact control for somite number ($P > 0.05$ by *t* test) and the pattern of *Pitx2* expression ($\chi^2 = 5.15$, $P > 0.1$ by 2×4 χ^2 test).

[d] 13 embryos were cohybridized with *T* riboprobe, 11 showed normal expression in axial tissues and 2 showed partially duplicated axial tissue (see Fig. 4I for an example).

[e] Significant difference from the intact control for somite number ($P < 0.02$ by *t* test) and *Pitx2* expression ($\chi^2 = 15.8$, $P < 0.02$ by 2×4 χ^2 test).

[f] 15 embryos were cohybridized with *T* riboprobe, 13 showed no expression and 1 each showed partial duplication and disjointed axial tissue.

embryos (Figs. 4C and 4L), but was found in the LPM of the right side (Fig. 4D), both sides (Fig. 4E), or neither side (not shown) in the other 53% of embryos. Embryos whose node was split showed similar randomized *Pitx2* expression in the LPM as the intact controls (Table 3, Split node). Although apparently more embryos showed the right LPM expression (Figs. 4F and 4M), the overall frequency of unilateral versus isomeric *Pitx2* expression does not differ significantly between the intact and the split-node controls. In the node-ablated embryo, there is significantly increased incidence of bilateral (Figs. 4H, 4I, and 4N) or the loss of *Pitx2* expression in the LPM (Fig. 4J). Only 14% of node-ablated embryos maintained unilateral (Fig. 4G) expression of the *Pitx2* activity in the LPM (Table 3, Node-ablated). In all the experimental embryos, *Pitx2* expression was maintained in the anterior neuroectoderm and the cranial mesoderm irrespective of the expression pattern in the LPM, suggesting that the heterotopic activity of the *Pitx2* gene is indicative of specific changes in the laterality of the embryonic tissue following node ablation.

DISCUSSION

Node Ablation Disrupts Left–Right Asymmetry of the Mouse Embryo at Early Organogenesis

During early organogenesis of the mouse embryo, the laterality of the body is revealed by the looping of the heart and the rotation of body axis (Kaufman and Navaratnam, 1981; Biben and Harvey, 1997; Miller and White, 1998) and the asymmetric expression of gene activity mostly in the tissues to the left of the body axis (King and Brown, 1999). From the early head-fold to the early-somite stage, transcripts of *Pitx2* (a member of the *bicoid* class homeodomain gene), *nodal*, and *lefty2* (both encoding TGFβ factors) are expressed in the left LPM (Collignon *et al.*, 1996; Meno *et*

FIG. 4. Expression of the *Pitx2* gene in the lateral plate mesoderm of intact embryos that developed *in vivo* (A, B, K) and *in vitro* (C–E, L) and of split-node (F, M) and node-ablated embryos (G–J, N) that were cultured *in vitro.* The *Pitx2* gene is expressed in the head folds and the left lateral plate mesoderm of embryos *in vivo* (A, three to four somite; B, eight somite). In embryos that were cultured for 24 h *in vitro*, *Pitx2* expression is found unilaterally either in the left (C, L) or in the right lateral plate mesoderm (D) or bilaterally (E). The node-split embryos show randomized expression of *Pitx2* activity including the ectopic expression in the right lateral plate mesoderm (F, M). The node-ablated embryos display ectopic *Pitx2* expression in the lateral plate mesoderm on the right (G) or on both sides (H, I, N). In some node-ablated embryos, no expression is seen in the anterior lateral plate mesoderm (J), but some weak expression is found in tissues next to the node. Specimens shown in C, I, J, and N were hybridized simultaneously for *Pitx2* and *T*, others were hybridized for *Pitx2* only. *T*-expressing axial tissue is present in the control embryos (C, M), but is disrupted (I) or absent (J, N) in the node-ablated embryos. Arrowheads, *Pitx2*-expressing tissue in lateral plate mesoderm; arrows, *T*-expressing axial tissues. A–J show the ventral view and K–N the *en face* view of the embryo. L, left-hand side; R, right-hand side. Bar, 100 (A–D) or 50 μm (E–H).

al., 1996; Ryan *et al.,* 1998; Piedra *et al.,* 1998). Asymmetric expression of the *nodal* gene is also detected in the endodermal cells adjacent to the node of the early head-fold stage embryo and *lefty1* is expressed on the left half of the floor plate, which is derivative of the node (Collignon *et al.,* 1996; Beddington and Robertson, 1999; Meno *et al.,* 1998). Changes in the expression patterns of these genes correlate well with the aberration in left–right asymmetry caused by mutation of genes involved in the TGFβ signaling (Collignon *et al.,* 1996; Oh and Li, 1997; Nomura and Li, 1998) and the loss of *Hnf3*β activity (Dufort *et al.,* 1998). The asymmetric expression of these genes at early organogenesis therefore heralds the establishment of the left–right pattern of morphogenesis.

In the present study, the expression of the *Pitx2* gene was examined to assess the laterality of the body plan in the experimental embryos. We found that in embryos that developed *in vitro* from late gastrulation to early-somite stage, *Pitx2* expression is randomized. Although the expression in the left LPM is maintained in about 50% of the embryos, ectopic expression of the *Pitx2* gene in the remaining embryos is found in the right LPM or bilaterally in both LPM, or it is completely lost. This randomized pattern of *Pitx2* expression in the LPM is reminiscent of the *Pitx2* expression in the *inversus viscerum* (*iv*)-mutant embryo (Ryan *et al.,* 1998; Piedra *et al.,* 1998) and of the *lefty2* gene in the KIF3B-deficient embryo (Nonaka *et al.,* 1998). Our finding raises two important issues regarding the timing and the role of the node in the specification of left–right asymmetry in the mouse embryo. The lability of the *Pitx2* expression suggests that although the laterality of the body plan may have been specified at early organogenesis, the pattern is not fully determined. A similar conclusion on the timing of determination of laterality has been drawn from teratological studies on rat embryos *in vitro.* Randomization of heart looping and body rotation can be induced by drug treatments most effectively at late gastrulation up to the early-head-fold stage (Fujinaga and Baden, 1991; McCarthy and Brown, 1998). In the chick embryo, the early asymmetric expression of genes (*Shh, nodal, ActRIIa, Act RIIb, activin* β*B*) in the node and the adjacent germ-layer tissue suggests that Hensen's node is important for the establishment of the laterality of the body plan (reviewed by Levin, 1997; Harvey, 1998). Although asymmetric activity of these genes (with the possible exception of *nodal*) is not found in the mouse node, recent studies have pointed to a possible involvement of the node in left–right patterning. Mutations of the *lrd* and the *kif3B* genes that lead to the loss of respectively the microtubule-associated dynein and motor protein associated with the cilia in the node cells (Supp *et al.,* 1997; Nonaka *et al.,* 1998) result in the randomization of body laterality. It is postulated that the disruption of these cytoskeletal proteins will affect the directional trafficking of morphogenetic signal and result in the loss of node function. Indeed, the disturbance of the ciliary activity of the node by exposing it to the artificial culture medium has been suggested to be the cause underlying the randomization of the laterality of the embryo that develops *in vitro* (Nonaka *et al.,* 1998).

The ablation of the node at late gastrulation has further disrupted the left–right pattern of the embryo and leads to the isomerism of the body axis. The majority of the node-ablated embryos have lost the asymmetric pattern of *Pitx2* expression and the LPM has acquired either an all-right or all-left characteristic. In the chick embryo, the signal(s) that determines the laterality of the axis resides initially in the LPM and is transferred to Hensen's node at the commencement of neurulation (Pagan-Westphal and Tabin, 1998). It has been shown that in *Xenopus,* the midline tissues such as the notochord and the floor plate may influence the asymmetrical expression of the *Xnr-1* gene in the LPM mainly by repressing gene expression in the right LPM (Lohr *et al.,* 1997, 1998). The impact of node ablation on the induction of isomerism in the mouse embryo is consistent with the instructive role of the node or its derivatives to maintain and stabilize the initial specification of the laterality of the body. The induction of isomerism in the laterality of the body axis is reminiscent of the loss of asymmetry in the *Hnf3*β mutant. No morphological recognizable node is formed and the notochord and floor plate are missing in the mutant embryo. *Nodal* expression is absent from the lateral plate mesoderm and *Lefty* expression is either absent or in both the left and the right lateral plate mesoderm (Collignon *et al.,* 1996; Dufort *et al.,* 1998). The loss of asymmetric gene activity is associated with absence of heart looping and body rotation (Dufort *et al.,* 1998). The loss of the notochord has also been associated with abnormal cardic morphogenesis in mutant zebrafish embryos (Danos and Yost, 1996). It is not known if the isomerism as revealed by *Pitx2* activity in the node-ablated embryo may have any effect on the morphogenesis of the heart and axis rotation. Mutation of the *No turning* genes results in similar disruption in the organization of the notochord (partial absence, duplication, and degeneration; Melloy *et al.,* 1998), suggesting that the primary effect of the mutation may be targeted to the node. It would be interesting to find out if the failure of axial rotation in the *No turning* mutant is associated with abnormal expression of genes such as *Pitx2, nodal,* or *lefty2* and if the node of the mutant embryo displays any loss in morphogenetic activity.

The Neural Axis Can Develop Autonomously in the Absence of Midline Tissues in the Node-Ablated Embryo

We have shown here that in most node-ablated embryos, the notochord is either absent or only partially formed in the trunk. However, no floor plate is present in the neural tube of these embryos even when a partial notochord is formed. The absence of floor plate differentiation might result from the loss of the floor plate progenitors which are not reconstituted from the cells recruited from the lateral germ layers and/or the lack of inductive activity of the disorganized notochord (Roelink *et al.,* 1994). Whether

other defects in dorsoventral patterning of the neural tube than the absence of an *Hnf3β*-expressing floor plate may be present in the notochord-deficient embryo is not known.

The absence of the node and its derivatives has no impact on the activity of the primitive streak to form the lateral and the paraxial mesoderm and to produce tissues for the extension of the neural tube. The ablation of the node, however, has resulted in the foreshortening of the anterior–posterior axis, the reduction in somite number, and the splitting of the axis in some node-ablated embryos. In some notochord-less embryos, the somites are less well organized and fused medially. It is not known if the dorsoventral delineation of sclerotome and dermamyotome may be affected by the absence of the notochord (Fan and Tessier-Lavigne, 1994).

Fate-mapping studies have shown that endodermal cells for the embryonic gut ingress through the node (Lawson *et al.*, 1986; Lawson and Pedersen, 1987; Tam and Beddington, 1992). The ablation of the node, however, does not affect the formation of mid- and hindgut endoderm. The absence of a node in *Hnf3β*-mutant embryo also does not affect the formation of the gut endoderm (Dufort *et al.*, 1998). This may suggest that the node is not the only site of endodermal recruitment or the sole source of the progenitor (Lawson *et al.*, 1991). Alternatively, the gut endoderm may have been recruited from other germ-layer tissues during the reconstitution of the axis. However, the lack of contribution of the dye-labeled cells to the endoderm in the present study indicated that they are unlikely to be recruited form the lateral germ-layer tissues.

The extent of axis elongation was not always related to the presence of the notochord; some embryos with no or partial notochord can develop an axis close to the normal length of an early-somite stage embryo. Despite the absence of a notochord, the neural tube still retains the proper anterior–posterior morphological and molecular characteristics and the neuroepithelium appears intact. The patterning of the anterior–posterior axis has been postulated to take place prior to gastrulation by the inductive interaction between the visceral endoderm and the epiblast (Thomas and Beddington, 1996; Beddington and Robertson, 1999; Knoetgen *et al.*, 1999). In the late gastrula, progenitor cells for the anterior neuroectoderm and the cranial mesoderm (Tam, 1989), and the midline mesendoderm that is derived from the early gastrula organizer and later forms the head process (Lawson *et al.*, 1991; Tam *et al.*, 1997b), are fully established in the ectoderm and mesoderm anterior to the node. It is therefore expected that development of the head structures will be unaffected by the ablation of the node which may be important for the patterning of the trunk structures (Camus and Tam, 1999). In the node-ablated embryo, the loss of neural tissues is replenished by the recruitment of cells from the lateral germ layers and the neural axis retains its anterior–posterior polarity. This suggests that by the late-gastrula stage, the patterning activity of the anterior visceral endoderm and the derivatives of the early gastrula organizer has already set into motion the necessary events required to pattern the neural axis, without further input from the node. Thus, signaling by the node in patterning the neural axis appears to be completed earlier in development than previously suggested (reviewed by Tam *et al.*, 1997a) and sustained node activity is not required to maintain this patterning. It would be interesting to determine whether the early gastrula organizer may play a more critical role in neural axis patterning. However, such an analysis is hampered by the difficulty in delineating the organizer population for surgical ablation at this stage because of the lack of morphological landmarks. Future experiment may require a genetic approach using conditional gene targeting to specifically delete the early organizer cells based upon their molecular properties.

The Mouse Embryo Does Not Reconstitute the Node after Ablation

In the chick embryo, normal differentiation of the notochord occurs after the removal of the tissue fragment containing the Hensen's node and the rostral segment of the primitive streak (Psychoyos and Stern, 1996). The cell populations that are involved in the reconstitution of the notochord have been localized to the blastoderm lateral to the Hensen's node and these cells, which display expression of the *Hnf3β* gene upon isolation, differentiate into notochord instead of neuroectoderm (Yuan and Schoenwolf, 1998). The *de novo* specification of the notochord in the lateral blastoderm seems to be regulated by an inductive interaction emanating from the tissue flanking the primitive streak (Yuan *et al.*, 1995a,b). In the present study, about 23% of the node-ablated embryos have formed a complete notochord. This may suggest that in the node-ablated embryos, the notochordal progenitors that have been ablated are reconstituted from the remaining embryonic cells. However, assaying for gene activity that is normally associated with the node of the late gastrula revealed that incomplete ablation of the node tissue may occur in about 21% of the node-ablated embryos examined immediately after ablation. When the node-ablated embryos were examined for gene expression at 5–6 h after ablation, about 26% of the embryos expressed *Hnf3β* and *Lim1* activity in the healed tissues at the anterior end of the primitive streak. The frequency of detecting residual gene activity is remarkably coincidental to the frequency of complete notochordal formation (23%) in the node-ablated embryos that were studied for the presence of *T*- *Hnf3β*- and *Shh*-expressing tissues in the midline tissue at the early-somite stage. It is likely that the apparent reconstitution of the notochord can be accounted for by the restoration of the notochordal progenitors through the compensatory proliferation and differentiation of the residual "node" cells in some node-ablated embryos. Therefore, in contrast to the situation in the avian embryo, there is no compelling evidence that any *de novo* regeneration of the notochordal progenitors has occurred in the mouse embryo following the ablation of the

node. This may place the mouse gastrula in the same league as the zebrafish and *Xenopus* embryos that also seem not to regenerate the notochord after the removal of the notochordal progenitors (Clark *et al.*, 1991; Cooke, 1985; Shih and Fraser, 1996).

The lack of reconstitution of the notochord in the mouse embryo may be due to the loss of the competence of the germ-layer tissues to do so by the late-gastrula stage. It has been possible to define regions of the blastoderm lateral to Hensen's node and the primitive streak in the avian embryo that are involved with the inductive interaction during the reconstitution of the notochord (Yuan *et al.*, 1995a,b). If a similar topographical relationship of inducing and responding regions is maintained in the mouse gastrula, cells immediately lateral to the node would correspond to the population that potentially can be respecified as the notochord progenitors. Results of the cell-tracing experiments show that the germ-layer tissues lateral to the ablated node can adopt a novel fate and colonize the neural tube. This entails the respecification of the development program and the adoption of a different pattern of morphogenetic cell movement. However, these cells contribute only infrequently to notochord-like structures. It is possible that the surgical manipulation performed in our study may have removed, in addition to the node, the tissues that correspond to the responding population that will reconstitute the notochord. This absence of tissues that may respond to signals of respecification may explain the lack of notochord reconstitution in the mouse compared with that observed in the avian embryo. However, such discrepancy between the species may be difficult to resolve unless a precise delineation of the interacting components similar to what has been accomplished with the chick gastrula (Psychoyos and Stern, 1996; Yuan *et al.*, 1995a,b; Yuan and Schoenwolf, 1998) can also be achieved with the mouse gastrula.

ACKNOWLEDGMENTS

We thank Siew-Lan Ang, Richard Behringer, Bernhard Herrmann, Juan Carlos Ipzisúa-Belmonte, Randy Johnson, Andy McMahon, Gail Martin, and Janet Rossant for gifts of riboprobes; Louise Cheng for technical assistance; and Peter Rowe for reading the manuscript. Our work is supported by the Human Frontier of Science Program (project grant to Richard Behringer, Siew-Lan Ang, Hiroshi Sasaki, and P.P.L.T.), the National Health and Medical Research Council (NH&MRC) of Australia, and Mr. James Fairfax. P.P.L.T. is an NH&MRC Principal Research Fellow.

REFERENCES

Ang, S.-L., and Rossant, J. (1994). *HNF-3β* is essential for node and notochord formation in mouse development. *Cell* **78,** 561–574.

Arendt, D., and Nübler-Jüng, K. (1997). Dorsal or ventral: Similarities in fate maps and gastrulation patterns in annelids, arthropods and chordates. *Mech. Dev.* **61,** 7–22.

Bally-Cuif, L., and Boncinelli, E. (1997). Transcription factors and head formation in vertebrates. *BioEssays* **19,** 127–135.

Beddington, R. S. P. (1994). Induction of a second neural axis by the mouse node. *Development* **120,** 613–620.

Beddington, R. S. P., and Robertson, E. J. (1999). Axis development and early asymmetry in mammals. *Cell* **96,** 195–209.

Biben, C., and Harvey, R. P. (1997). Homeodomain factor *Nkx2.5* controls left–right asymmetric expression of bHLH gene *eHand* during murine heart development. *Genes Dev.* **11,** 1357–1369.

Camus, A., and Tam, P. P. L. (1999). The organizer of the gastrulating mouse embryo. *Curr. Top. Dev. Biol.* **45,** 117–153.

Chiang, C., Litingtung, Y., Lee, E., Young, K. E., Corden, J. L., Westphal, H., and Beachy, P. A. (1996). Cyclopia and defective axial patterning in mice lacking *Sonic hedgehog* gene function. *Nature* **383,** 407–413.

Clarke, J. D. W., Holder, N., Soffe, S. R., and Storm-Mathisen, J. (1991). Neuroanatomical and functional analysis of neural tube formation in notochordless *Xenopus* embryos: Laterality of the ventral spinal cord is lost. *Development* **112,** 499–516.

Collignon, J., Varlet, I., and Robertson, E. J. (1996). Relationship between asymmetric nodal expression and the direction of embryonic turning. *Nature* **381,** 155–161.

Conlon, F. L., Wright, C. V. E., and Robertson, E. J. (1995). Effects of the T^{wis} mutation on notochord formation and mesodermal patterning. *Mech. Dev.* **49,** 201–210.

Cooke, J. (1985). Dynamics of the control of body pattern in the development of *Xenopus laevis*. II. Timing and pattern after u.v. irradiation of the egg and after excision of presumptive head endo-mesoderm. *J. Embryol. Exp. Morphol.* **88,** 135–150.

Danos, M. C., and Yost, H. J. (1996). Role of notochord in specification of cardiac left–right orientation in zebrafish and *Xenopus*. *Dev. Biol.* **177,** 96–103.

Dias, M. S., and Schoenwolf, G. C. (1990). Formation of ectopic neuroepithelium in chick blastoderms: Age-related capacities for induction and self-differentiation following transplantation of quail Hensen's nodes. *Anat. Rec.* **229,** 437–448.

Downs, K., and Davies, T. (1993). Staging of gastrulating mouse embryos by morphological landmarks in the dissecting microscope. *Development* **118,** 1255–1266.

Dufort, D., Schwartz, L., Harpal, K., and Rossant, J. (1998). The transcription factor HNF3β is required in visceral endoderm for normal primitive streak morphogenesis. *Development* **125,** 3015–3025.

Fan, C. M., and Tessier-Lavigne, M. (1994). Patterning of mammalian somites by surface ectoderm and notochord: Evidence of sclerotome induction by a hedgehog homolog. *Cell* **79,** 1175–1186.

Fujinaga, M., and Baden, J. M. (1991). Critical period of rat development when sidedness of asymmetric body structures is determined. *Teratology* **44,** 453–462.

Gilbert, S. F., and Saxen, L. (1993). Spemann's organizer: Models and molecules. *Mech. Dev.* **41,** 73–89.

Harland, R., and Gerhart, J. (1997). Formation and function of Spemann's organizer. *Annu. Rev. Cell Dev. Biol.* **13,** 611–667.

Harvey, R. P. (1998). Links in the left–right axial pathway. *Cell* **94,** 273–276.

Herrmann, B. G. (1995). The mouse *Brachyury (T)* gene. *Semin. Dev. Biol.* **6,** 385–394.

Ho, R. K. (1992). Axis formation in the embryo of the zebrafish, *Brachydanio rerio*. *Semin. Dev. Biol.* **3,** 53–64.

Izpisúa-Belmonte, J. C., De Robertis, E. M., Storey, K. G., and Stern, C. D. (1993). The homebox gene *goosecoid* and the origin of organizer cells in the early chick blastoderm. *Cell* **74,** 645–659.

Kaufman, M. H., and Navaratnam, V. (1981). Early differentiation of the heart in mouse embryos. *J. Anat.* **133,** 235–246.

King, T., and Brown, N. A. (1999). Embryonic asymmetry: The left side gets all the best genes. *Curr. Biol.* **9,** R18–R22.

Knoetgen, H., Viebahn, C., and Kessel, M. (1999). Head induction in the chick by primitive endoderm of mammalian, but not avian origin. *Development* **126,** 815–825.

Lawson, K. A., and Pedersen, R. A. (1987). Cell fate, morphogenetic movement and population kinetics of embryonic endoderm at the time of germ layer formation in the mouse. *Development* **101,** 627–652.

Lawson, K. A., and Pedersen, R. A. (1992). Clonal analysis of cell fate during gastrulation and early neurulation in the mouse. *In* "Postimplantation Development in the Mouse," Ciba foundation Symposium, Vol. 165, pp. 3–26. Wiley, Chichester, UK.

Lawson, K. A., Meneses, J. J., and Pedersen, R. A. (1986). Cell fate and cell lineage in the endoderm of the presomite mouse embryo, studied with an intracellular tracer. *Dev. Biol.* **115,** 325–339.

Lawson, K. A., Meneses, J. J., and Pedersen, R. A. (1991). Clonal analysis of epiblast fate during germ layer formation in the mouse embryo. *Development* **113,** 891–911.

Lemaire, P., and Kodjabachian, L. (1996). The vertebrate organizer: Structure and molecules. *Trends Genet.* **12,** 525–532.

Levin, M. (1997). Left–right asymmetry in vertebrate embryogenesis. *BioEssays* **19,** 287–296.

Lohr, J. L., Danos, M. C., and Yost, H. J. (1997). Left–right asymmetry of a *nodal*-related gene is regulated by dorso-anterior midline structures during *Xenopus* development. *Development* **124,** 1465–1472.

Lohr, J. L., Danos, M. C., Grith, T. W., and Yost, H. J. (1998). Maintenance of asymmetric *nodal* expression in *Xenopus laevis*. *Dev. Genet.* **23,** 194–202.

McCarthy, A., and Brown, N. A. (1998). Specification of left–right asymmetry in mammals: Embryo culture studies of stage of determination and relationships with morphogenesis and growth. *Reprod. Toxicol.* **12,** 177–184.

Melloy, P. G., Ewart, J. L., Cohen, M. F., Desmond, M. E., Kuehn, M., and Lo, C. W. (1998). *No turning*, a mouse mutation causing left–right and axial patterning defects. *Dev. Biol.* **193,** 77–89.

Meno, C., Saijoh, Y., Gujii, H., Ikeda, M., Yokoyama, T., Yokoyama, M., Toyoda, Y., and Hamada, H. (1996). Left–right asymmetric expression of the TGF beta-family member lefty in mouse embryos. *Nature* **381,** 151–155.

Miller, S. A., and White, R. D. (1998). Right–left asymmetry of cell proliferation predominates in mouse embryos undergoing clockwise axial rotation. *Anat. Rec.* **250,** 103–108.

Nomura, M., and Li, E. (1998). Smad2 role in mesoderm formation, left–right patterning and craniofacial development. *Nature* **393,** 786–790.

Nonaka, S., Tanaka, Y., Okada, Y., Takeda, S., Harada, A., Kanai, Y., Kido, M., and Hirokawa, N. (1998). Randomization of left–right asymmetry due to loss of nodal cilia generating leftward flow of extraembryonic fluid in mice lacking KIF3B motor protein. *Cell* **95,** 829–837.

Oh, S. P., and Li, E. (1997). The signaling pathway mediated by the type IIB activin receptor controls axial patterning and lateral asymmetry in the mouse. *Genes Dev.* **11,** 1812–1826.

Pagan-Westphal, S. M., and Tabin, C. J. (1998). The transfer of left–right positional information during chick embryogenesis. *Cell* **93,** 25–35.

Piedra, M. E., Icardo, J. M., Albajar, M., Rodriguez-Rey, J. C., and Ros, M. A. (1998). *Pitx2* participates in the late phase of the pathway controlling left–right asymmetry. *Cell* **94,** 319–324.

Psychoyos, D., and Stern, C. D. (1996). Restoration of the organizer after radical ablation of Hensen's node and the anterior end of the primitive streak in the chick embryo. *Development* **122,** 3263–3273.

Rashbass, P., Wilson, V., Rosen, B., and Beddington, R. S. (1994). Alterations in gene expression during mesoderm formation and axial patterning in *Brachyury (T)* embryos. *Int. J. Dev. Biol.* **38,** 35–44.

Roelink, H., Augsburger, A., Heemskerk, J., Korzh, V., Norlin, S., Ruiz i Altaba A., Tanabe, Y., Placezek, M., Edlund, T., Jessell, T. M., and Dodd, J. M. (1994). Floor plate and motor neuron induction by *vhh-1*, a vertebrate homolog of *hedgehog* expressed by the notochord. *Cell* **76,** 761–775.

Ryan, A. K., Blumberg, B., Rodriguez-Esteban, C., Yonei-Tamura, S., Tamura, K., Tsukui, T., de la Pena, J., Sabbagh, W., Greenwald, J., Choe, S., Norris, D. P., Robertson, E. J., Evans, R. M., Rosenfeld, M. G., and Izpisúa-Belmonte, J. C. (1998). *Pitx2* determines left–right asymmetry of internal organs in vertebrates. *Nature* **394,** 545–551.

Slack, J. M. W. (1994). The why and whereforces of gastrulation. *Semin. Dev. Biol.* **5,** 69–76.

Shih, J., and Fraser, S. E. (1996). Characterizing the zebrafish organizer: Microsurgical analysis at the early-shield stage. *Development* **122,** 1313–1322.

Snow, M. H. L. (1981). Autonomous development of parts isolated from primitive-streak-stage mouse embryo. Is development clonal? *J. Embryol. Exp. Morphol.* **65**(Suppl.), 269–287.

Spemann, H., and Mangold, H. (1924). Über induktion von Embryonalanlagen durch Implantation artfremder Organisatoren. *Roux Arch. Entwicklungsmech. Org.* **100,** 599–638.

Storey, K. G., Crossley, J. M., De Robertis, E. M., Norris, W. E., and Stern, C. D. (1992). Neural induction and regionalisation in the chick embryo. *Development* **114,** 729–741.

Sturm, K. A., and Tam, P. P. L. (1993). Isolation and culture of whole postimplantation embryos and germ layer derivatives. *Methods Enzymol.* **225,** 164–190.

Sulik, K., Dehart, D. B., Inagaki, T., Carlson, J. L., Vrablic, T., Gesteland, K., and Schoenwolf, G. C. (1994). Morphogenesis of the murine node and notochordal plate. *Dev. Dyn.* **201,** 260–278.

Supp, D., Witte, D., Potter, S., and Brueckner, M. (1997). Mutation of an axonemal dynein affects left–right asymmetry in *inversus viscerum* mice. *Nature* **389,** 963–966.

Tam, P. P. L. (1989). Regionalisation of the mouse embryonic ectoderm: Allocation of prospective ectodermal tissues during gastrulation. *Development* **101,** 55–67.

Tam, P. P. L., and Beddington, R. S. P. (1987). The formation of mesodermal tissues in the mouse embryo during gastrulation and early organogenesis. *Development* **99,** 109–126.

Tam, P. P. L., and Beddington, R. S. P. (1992). Establishment and organization of germ layers in the gastrulating mouse embryo. *In* "Postimplantation Development in the Mouse," Ciba Foundation Symposium, Vol. 165, pp. 27–49. Wiley, Chichester, UK.

Tam, P. P. L., and Behringer, R. R. (1997). Mouse gastrulation: The formation of the mammalian body plan. *Mech. Dev.* **68,** 3–25.

Tam, P. P. L., and Quinlan, G. A. (1996). Mapping vertebrate embryos. *Curr. Biol.* **6,** 106–108.

Tam, P. P. L., Quinlan, G. A., and Trainor, P. A. (1997a). The patterning of progenitor tissues for the cranial region of the

mouse embryo during gastrulation and early organogenesis. *Adv. Dev. Biol.* **5,** 137–200.

Tam, P. P. L., Steiner, K. A., Zhou, S. X., and Quinlan, G. A. (1997b). Lineage and functional analysis of the mammalian organizer. *Cold Spring Harbor Symp. Quant. Biol.* **62,** 135–144.

Thomas, P., and Beddington, R. S. P. (1996). Anterior primitive endoderm may be responsible for patterning the anterior neural plate in the mouse embryo. *Curr. Biol.* **6,** 1487–1496.

Weinstein, D. C., Ruiz i Altaba, A., Chen, W. S., Hoodless, P., Prezioso, V. R., Jessell, T. M., and Darnell, J. E., Jr. (1994). The winged-helix transcription factor HNF-3 beta is required for notochord development in the mouse embryo. *Cell* **78,** 575–588.

Wilkinson, D. G., and Nieto, M. A. (1993). Detection of messenger RNA by in situ hybridization to tissues sections and whole mounts. *Methods Enzymol.* **225,** 361–373.

Yuan, S., and Schoenwolf, G. C. (1998). De novo induction of the organizer and formation of the primitive streak in an experimental model of notochord reconstitution in avian embryos. *Development* **125.**

Yuan, S., Darnell, D. K., and Schoenwolf, G. C. (1995a). Mesodermal patterning during avian gastrulation and neurulation: Experimental induction of notochord from non-notochordal precursor cells. *Dev. Genet.* **17,** 38–54.

Yuan, S., Darnell, D. K., and Schoenwolf, G. C. (1995b). Identification of inducing, responding, and suppressing regions in an experimental model of notochord formation in avian embryos. *Dev. Biol.* **172,** 567–584.

Received for publication December 18, 1998
Revised March 16, 1999
Accepted March 16, 1999